https://doi.org/10.5194/egusphere-2026-2206
Preprint. Discussion started: 4 May 2026


# Hydrological implications of vegetation-associated precipitation recycling during peak growing season over the Loess Plateau

Jiaxiang Deng[1], Quan Quan[1], Shuangcheng Tang[2], Hanbo Yang[3], and Xiaoyu Song[1]
[1]State Key Laboratory of Water Engineering Ecology and Environment in Arid Area, Xi'an University of Technology, Xi'an, China
[2]College of Hydraulic Science and Engineering, Yangzhou University, Yangzhou, China
[3]Tsinghua University, Beijing, China

*Correspondence to*: Quan Quan (qq@xaut.edu.cn)

**Abstract.** Vegetation restoration on the Loess Plateau has led to continued debate over whether enhanced land–atmosphere coupling can meaningfully alleviate water scarcity in this water-limited region. In this study, we combined the WAM-2layers atmospheric moisture-tracking model with a random forest–enhanced Budyko framework and introduced a vegetation-weighted leaf area index ($LAI_w$) to examine vegetation-associated precipitation recycling and its hydrological implications during the peak growing season (July–August) from 2000 to 2022. Precipitation over the Loess Plateau is dominated by land-sourced moisture, which accounts for 86.5% of total precipitation. Internal moisture recycling contributes 14.4% of total precipitation and shows a declining trend of −0.073 mm $yr^{-1}$. Surface water availability also declines significantly, at a rate of −0.34 mm $yr^{-1}$, mainly because evapotranspiration increases by 0.31 mm $yr^{-1}$. At the regional mean scale, vegetation-associated recycled precipitation makes only a limited contribution to precipitation, evapotranspiration, and surface water availability, accounting for 0.059%, 0.02%, and 0.107%, respectively. This low net contribution partly reflects the fact that internal moisture recycling itself represents only a limited fraction of total precipitation, and that positive and negative vegetation-associated effects partly offset each other. However, the hydrological effect varies clearly along the $LAI_w$ gradient, with weak positive contributions under low vegetation density and increasingly negative contributions under high vegetation density. These findings suggest that under water-limited conditions, enhanced vegetation–atmosphere coupling does not necessarily lead to meaningful gains in surface water availability. This seasonal focus is intended to capture the period of strongest vegetation–atmosphere coupling rather than the full annual water balance.

## 1 Introduction

Water scarcity and ecological fragility are major constraints on sustainable development in arid and semi-arid regions worldwide (Kummu et al., 2016; He et al., 2021). Climate warming has intensified the hydrological cycle by altering evaporation and precipitation processes, thereby reshaping regional water availability and increasing hydroclimatic risks, especially in water-limited environments (Giorgi et al., 2014; Huang et al., 2016; Wang et al., 2023; Zhang et al., 2023). Although enhanced moisture recycling may partly mitigate water stress by returning evapotranspired water to the land surface

https://doi.org/10.5194/egusphere-2026-2206
Preprint. Discussion started: 4 May 2026


as precipitation, the extent to which this process can effectively alleviate regional water limitation remains insufficiently understood.

Atmospheric moisture transport plays a fundamental role in regulating regional precipitation and water availability (Dominguez et al., 2020; He et al., 2021). Precipitation over a given region may originate either from evapotranspiration within the region through internal moisture recycling or from moisture advected from upwind source areas (van der Ent et al., 2010; Tuinenburg et al., 2022; Cui et al., 2022). The balance between these internal and external moisture sources is particularly important in arid and semi-arid regions, where water availability is highly sensitive to both land–atmosphere coupling and atmospheric circulation (Te Wierik et al., 2022; Li et al., 2023; Zhang et al., 2022). Therefore, quantifying the contribution of local evapotranspiration to regional precipitation is essential for understanding whether land-surface changes can meaningfully influence regional water resources.

The Loess Plateau (LP) of China is a representative water-limited region that has experienced severe ecological degradation and long-term water stress (Huang et al., 2016; Huang et al., 2017). Since the implementation of large-scale ecological restoration programs around 2000, vegetation cover and ecosystem productivity have increased substantially across the region (Li et al., 2021; Li et al., 2022). However, the hydrological consequences of vegetation restoration remain debated. On the one hand, vegetation recovery can increase evapotranspiration, intensify soil moisture depletion, and reduce runoff, thereby aggravating water scarcity (Feng et al., 2016; Deng et al., 2020; Zhang et al., 2018). On the other hand, stronger evapotranspiration may enhance land–atmosphere coupling, promote atmospheric moisture recycling, and potentially increase precipitation (Yosef et al., 2018; Zhang et al., 2022a; Wei et al., 2019). These competing effects raise a key but unresolved question: under water-limited conditions, can vegetation-associated precipitation recycling provide a meaningful hydrological benefit, or is it largely offset by the additional water consumption associated with vegetation growth?

The seasonal timing of moisture recycling analysis requires careful consideration in dryland regions. While the full growing season on the Loess Plateau spans June to September, previous studies indicate that vegetation-atmosphere coupling intensity varies substantially within this period. July and August represent the peak growing season, when leaf area index reaches its annual maximum, solar radiation is strongest, and soil moisture remains favorable for active evapotranspiration (Wang et al., 2019; Li et al., 2024). During this period, transpiration accounts for the dominant fraction of evapotranspiration and land–atmosphere moisture exchange is most pronounced (Guo et al., 2025). Consequently, focusing on July–August allows targeted assessment of vegetation-associated hydrological effects when they are expected to be strongest. This approach follows established practices in moisture recycling research where seasonal subsets are analyzed to isolate specific process periods (Zemp et al., 2014).

Addressing this question requires linking vegetation dynamics, evapotranspiration, atmospheric moisture tracking, and regional water balance within a unified framework. Existing studies have provided important insights into either the hydrological costs of revegetation or the climatic effects of land–atmosphere feedbacks, but quantitative assessments that explicitly connect vegetation-associated moisture recycling to regional water availability remain limited. In particular, few studies have integrated atmospheric moisture tracking with water-balance analysis to evaluate whether the precipitation

https://doi.org/10.5194/egusphere-2026-2206
Preprint. Discussion started: 4 May 2026


returned through vegetation-related recycling is large enough to compensate for the accompanying evapotranspiration increase in dryland ecosystems.

The Budyko framework provides a widely used basis for evaluating climatic controls on water partitioning between evapotranspiration and runoff (Budyko, 1974). However, its conventional form generally assumes long-term equilibrium conditions and fixed catchment characteristics, which may be insufficient for regions such as the Loess Plateau, where hydroclimatic conditions are spatially heterogeneous and land-surface properties have changed substantially under ecological restoration (Yang et al., 2009; Yokoo et al., 2008; Woods, 2003; Yang et al., 2015). To better capture these variations, it is necessary to allow the effective catchment parameter to vary with vegetation, soil moisture, and meteorological conditions.

In this study, we develop an integrated framework that combines the WAM-2layers atmospheric moisture tracking model with a random forest–enhanced Budyko approach to quantify vegetation-associated precipitation recycling and its hydrological implications over the Loess Plateau during the peak growing season (July–August) from 2000 to 2022. We further introduce a vegetation-weighted indicator, $LAI_w$, as a diagnostic measure that combines vegetation structure with relative evapotranspiration intensity in order to represent vegetation conditions more closely related to land–atmosphere moisture exchange. Specifically, this study aims to (1) characterize the spatiotemporal patterns of growing-season moisture recycling and water availability over the Loess Plateau, (2) quantify the vegetation-associated component of recycled precipitation, and (3) evaluate whether this recycled precipitation meaningfully offsets evapotranspiration-induced water losses under different vegetation-density conditions. By doing so, this study seeks to clarify the hydrological limits of vegetation-associated precipitation recycling in a water-constrained dryland region.

## 2 Data and methods

### 2.1 Study area and climatic characteristics

The Loess Plateau (LP) is located in the middle reaches of the Yellow River basin (33°43′–41°16′N, 104°54′–114°33′E) and represents a typical arid and semi-arid region in northern China. The region covers an area of approximately 640,000 km² and is characterized by complex topography, with elevation generally decreasing from northwest to southeast and an overall elevation range exceeding 3000 m. The Loess Plateau is dominated by a temperate continental monsoon climate. The mean annual air temperature and precipitation are approximately 9.4 °C and 593.7 mm, respectively. Precipitation exhibits strong seasonality, with about 60–70% of the annual total occurring between June and September, whereas winter precipitation is limited and contributes negligibly to the annual water budget (Wang et al., 2023). Under the influence of the East Asian monsoon system, precipitation over the Loess Plateau also shows pronounced interannual variability, with wet years receiving several times more precipitation than dry years and extreme rainfall events occurring frequently (Liu et al., 2025).

Given the strong seasonality of both precipitation and vegetation activity, this study focuses on July and August as the primary analysis period. These two months correspond to the peak growing season on the Loess Plateau, during which leaf area index (*LAI*) and fractional vegetation cover generally reach their annual maxima, solar radiation is relatively strong, and soil moisture

https://doi.org/10.5194/egusphere-2026-2206
Preprint. Discussion started: 4 May 2026


conditions remain favorable for active land–atmosphere exchange. As a result, evapotranspiration and vegetation–atmosphere interactions are most pronounced during this period (Wang et al., 2019; Li et al., 2024; Guo et al., 2025). Focusing on July and August therefore allows this study to better capture the period when vegetation-related moisture recycling is expected to be strongest, providing a targeted basis for evaluating vegetation-associated hydrological effects during the peak growing season

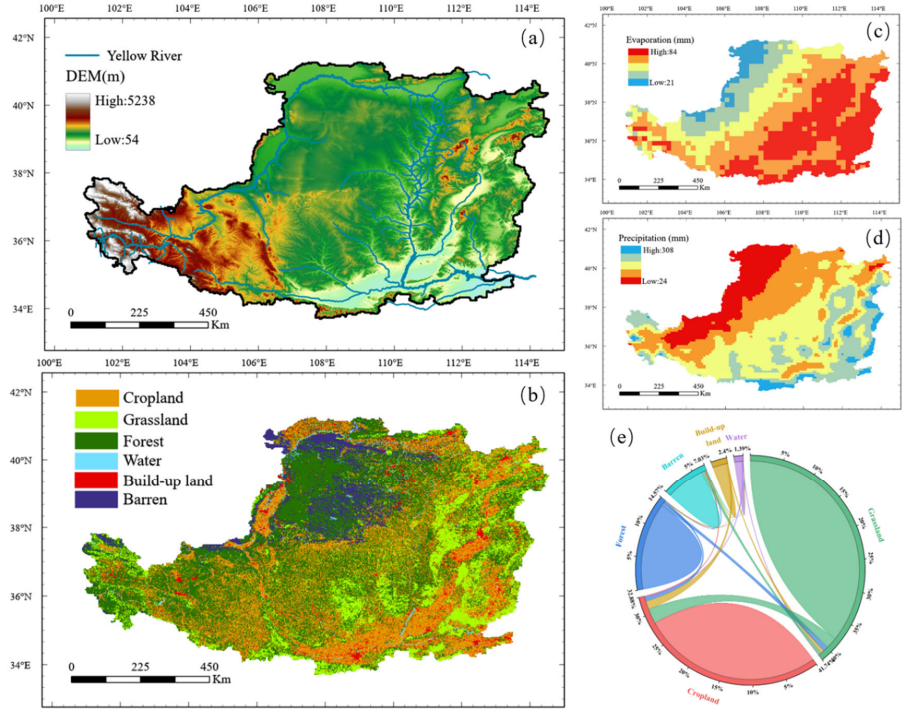


in this water-limited region. This seasonal focus is intended to isolate the period of strongest vegetation–atmosphere coupling rather than to represent the full annual water balance.

**Figurer. 1: Study area and key characteristics, including (a) topography and river network, (b) land cover, (c) evaporation, (d) precipitation, and (e) land-cover conversions.**

## 2.2 Data

Monthly evapotranspiration (*ET*) and potential evapotranspiration ($ET_0$) data for July and August during 2000–2022 were obtained from the Global Land Evaporation Amsterdam Model (GLEAM, v3.6a) dataset, with a spatial resolution of 0.25° (Martens et al., 2017). GLEAM ET has been extensively evaluated against eddy covariance (*EC*) observations across China and shows good agreement at the monthly scale, with an average correlation coefficient of 0.86 (Yang et al., 2017).

https://doi.org/10.5194/egusphere-2026-2206
Preprint. Discussion started: 4 May 2026


Monthly precipitation data for July and August during 2000–2022 were derived from the ERA5 reanalysis dataset at a spatial resolution of 0.25° (Hersbach et al., 2020). ERA5 precipitation has been shown to capture the annual and seasonal variability of observed precipitation over China reasonably well (Jiao et al., 2021) and exhibits a strong correlation (r = 0.92) with official national statistics at the 99% confidence level (An et al., 2025). Before subsequent analyses, the ERA5 precipitation and GLEAM ET datasets were temporally aligned for July–August during 2000–2022 and resampled to a common 0.25° grid using nearest-neighbor interpolation to ensure spatial consistency.

For atmospheric moisture tracking, hourly meteorological variables from the ERA5 dataset were collected for June–August during 2000–2022. These variables included air temperature, precipitation, specific humidity, wind components, surface pressure, dew-point temperature, total column water vapor, and surface evaporation. Specific humidity and wind fields were extracted for 17 vertical pressure levels ranging from 1000 to 100 hPa, all at a spatial resolution of 0.25°. ERA5 data have been widely used in previous moisture-tracking studies over China and have shown robust performance (An et al., 2025; Xie et al., 2024; Zhang et al., 2024). Considering the atmospheric residence time of water vapor (van der Ent et al., 2013), meteorological data from June were included as auxiliary input to enable more complete tracking of the moisture contributing to precipitation in July and August.

Vegetation conditions were characterized using the High-Quality Leaf Area Index (HiQ-LAI) dataset, a globally consistent *LAI* product derived from MODIS LAI Collection 6.1 using a spatiotemporal information compositing algorithm (STICA) (Yan et al., 2024). Compared with the original MODIS LAI product, HiQ-LAI improves temporal stability and spatial consistency by integrating pixel-level quality information and spatiotemporal correlations while preserving the underlying radiative transfer framework. The dataset provides global coverage at an 8-day temporal resolution and a spatial resolution of 5 km for 2000–2022, and has been validated against ground-based observations, showing reduced noise and improved phenological consistency relative to the original MODIS LAI. In this study, HiQ-LAI data for July and August were extracted and aggregated to characterize vegetation conditions during the peak growing season over the Loess Plateau. The HiQ-LAI dataset is publicly available via Zenodo (Yan et al., 2023).

Additional variables used in the random forest modeling of the Budyko parameter $n$ were derived from the ERA5-Land and ERA5 reanalysis datasets. Four-layer soil water content (swvl1–swvl4), near-surface wind components ($u$ and $v$), and surface temperature were obtained from ERA5-Land at a spatial resolution of 0.1°. Surface runoff (*src*) and surface shortwave radiation (*ssr*) were obtained from the ERA5 hourly single-level dataset at a spatial resolution of 0.25°. Vegetation cover (*VC*) was characterized using the China regional fractional vegetation cover (*FVC*) dataset at 250 m resolution (Gao et al., 2024). All variables were spatially aggregated to a common 0.25° grid to maintain consistency with the Budyko framework.

### 2.3 Methodology

This study employs an integrated framework combining atmospheric moisture tracking, vegetation-based diagnostics, and hydrological modeling to examine vegetation-associated precipitation recycling and its hydrological implications over the Loess Plateau during the peak growing season (Fig. 2a).

https://doi.org/10.5194/egusphere-2026-2206
Preprint. Discussion started: 4 May 2026


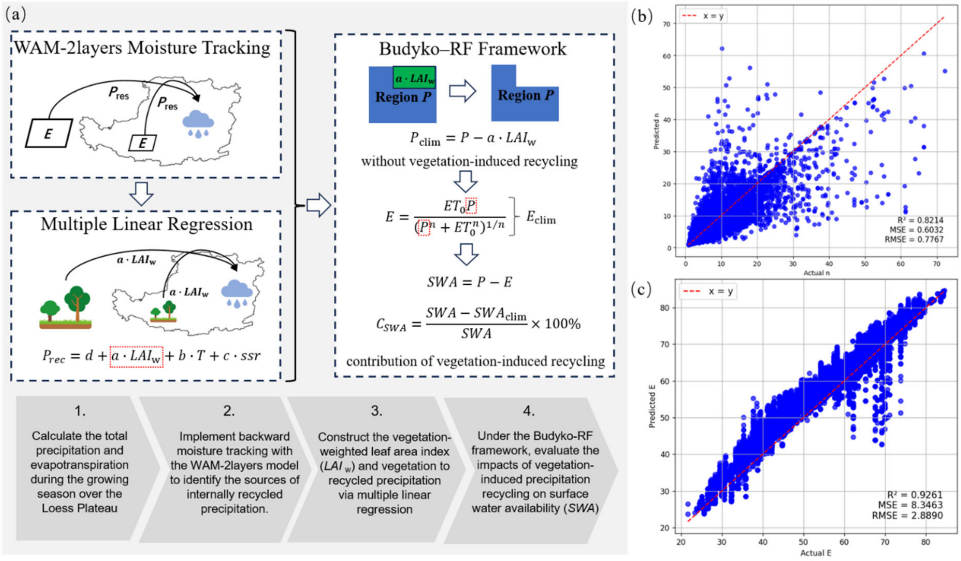


**Figure. 2: Methodological framework and model validation results, including (a) schematic diagram of the methodological framework, (b) scatter plot of predicted n values from the random forest model versus observed n values in the test set, and (c) scatter plot of evapotranspiration estimated by the Budyko–RF framework versus observed evapotranspiration.**

### 2.3.1 Moisture tracking and precipitation source attribution

To identify the moisture sources of precipitation over the Loess Plateau (LP) and to separate the contributions from internal recycling and external advection, we employed the Eulerian moisture-tracking model WAM-2layers v3 (Kalverla et al., 2025; van der Ent et al., 2013, 2014). The model partitions the atmosphere into two layers, namely a lower layer ($k$=1) below approximately 812 hPa and an upper layer ($k$=0) representing the free atmosphere, and assumes that moisture is well mixed within each layer. In the model, tagged moisture is defined as $S^*=cS$, where $c$ is the tagged moisture concentration. Its spatiotemporal evolution is governed by the tagged moisture budget equation:

$$\frac{\Delta_t S^*}{\Delta t} + \frac{1}{A}\left(\Delta_x F_x^* + \Delta_y F_y^* + \Delta_p F_p^*\right) = E^* - P^* \quad (1)$$

where $S^*$ is tagged moisture storage, $F^*_x$, $F^*_y$, and $F^*_p$ are the tagged moisture fluxes in the zonal, meridional, and vertical directions, respectively, and $E^*$ and $P^*$ are the tagged evaporation and precipitation terms. In WAM-2layers, tagged horizontal fluxes are assumed to be proportional to total moisture fluxes, whereas the vertical tagged flux includes an additional dispersion term to enhance interlayer mixing. The vertical transport term is treated as a closure term representing exchange at the interface between the two layers.

https://doi.org/10.5194/egusphere-2026-2206
Preprint. Discussion started: 4 May 2026


For the two-layer implementation, evaporation is assigned entirely to the lower layer, whereas precipitation is partitioned between the upper and lower layers according to their relative moisture contents. The resulting upper- and lower-layer equations can be written as:

$$S_{ij,0}^{t+1} = S_{ij,0}^{t} + \Delta t \left[ -\frac{\left(F^{*}_{x,i+\frac{1}{2},j,0} - F^{*}_{x,i-\frac{1}{2},j,0}\right)}{A} - \frac{\left(F^{*}_{y,i,j+\frac{1}{2}0} - F^{*}_{y,i,j-\frac{1}{2}0}\right)}{A} - \frac{\left(F^{*}_{p,ij,\frac{1}{2}} + k_{vf}\left|F_{p,ij,\frac{1}{2}}\right|\left(c^{t}_{ij,1} - c^{t}_{ij,0}\right)\right)}{A} - c_{ij,0}\frac{S_{ij,0}}{S_{ijT}}P_{ij}^{t+\frac{1}{2}} \right] \quad (2)$$

and

$$S_{ij,1}^{t+1} = S_{ij,1}^{t} + \Delta t \left[ -\frac{\left(F^{*}_{x,i+\frac{1}{2},j,1} - F^{*}_{x,i-\frac{1}{2},j,1}\right)}{A} - \frac{\left(F^{*}_{y,i,j+\frac{1}{2}1} - F^{*}_{y,i,j-\frac{1}{2}1}\right)}{A} + \frac{\left(F^{*}_{p,ij,\frac{1}{2}} + k_{vf}\left|F_{p,ij,\frac{1}{2}}\right|\left(c^{t}_{ij,1} - c^{t}_{ij,0}\right)\right)}{A} + \delta_{e}F_{ij}^{t+\frac{1}{2}} - c_{ij,1}\frac{S_{ij,1}}{S_{ijT}}P_{ij}^{t+\frac{1}{2}} \right] \quad (3)$$

where $A$ is grid-cell area, $S_{ijT}$ is total column moisture, and $k_{vf}$ is the vertical dispersion coefficient. This two-layer formulation improves the representation of vertical moisture exchange relative to single-layer models, particularly under strong vertical wind shear.

In this study, WAM-2layers was run in backward-tracking mode to trace the sources of precipitation over the LP during July–August for 2000–2022. Considering the atmospheric residence time of water vapor, June meteorological inputs were also included, and the tracking period was set to July–August to ensure more complete tracing of moisture contributing to July–August precipitation. Hourly ERA5 variables were temporally interpolated to a 10 min time step and simulated at 0.25° spatial resolution. This configuration follows the model recommendation that moisture transport within a time step should not exceed one grid cell, thereby maintaining numerical stability under the Courant-Friedrichs-Lewy criterion.

Based on the tracking results, precipitation over the LP was decomposed into internally recycled and externally advected components, and the relative contributions of land and ocean source regions were quantified. The recycling ratio $\alpha$ is defined as (van der Ent et al., 2010):

$$\alpha = \frac{P_{v0}}{P_{v}} \quad (4)$$

where $P_v$ is the total precipitation over the LP during the tracking period, and $P_{v0}$ is the amount of precipitation over the LP that originates from evaporation within the LP and subsequently returns to the LP through atmospheric moisture transport.

### 2.3.2 Construction of LAIw and vegetation-associated component of recycled precipitation

To characterize vegetation conditions that are more directly related to land–atmosphere moisture exchange, a vegetation-weighted index, denoted as $LAI_w$, was constructed in this study. The purpose of this index is not to define a new physical state

https://doi.org/10.5194/egusphere-2026-2206
Preprint. Discussion started: 4 May 2026


variable, but to provide a diagnostic indicator that better links vegetation structure to the evaporative conditions under which atmospheric moisture recycling occurs.

Leaf area index (*LAI*) is widely used to represent vegetation canopy structure, but *LAI* alone does not fully reflect the extent to which vegetation is actively coupled to atmospheric moisture exchange. Under dryland conditions, the hydrological role of vegetation depends not only on canopy density, but also on the contemporaneous evaporative intensity associated with available water and energy. Grid cells with similar *LAI* may therefore contribute differently to moisture recycling if their evapotranspiration rates differ substantially. To account for this combined control, *LAI* was weighted by normalized actual evapotranspiration, so that vegetation in grid cells with stronger evapotranspiration receives greater emphasis in the subsequent diagnosis of recycled precipitation.

For each grid cell, the mean leaf area index during the peak growing season (July–August) was derived from the HiQ-LAI dataset. Actual evapotranspiration during the same period, denoted as $E_{obs}$, was used to represent the evaporative strength associated with local vegetation and hydroclimatic conditions. The vegetation-weighted index is defined as:

$$LAI_{w} = LAI \cdot \frac{E_{obs}}{\bar{E}_{obs}} \tag{5}$$

where $E_{obs}$ is the observed evapotranspiration at the grid scale, and $\bar{E}_{obs}$ is the spatial mean of $E_{obs}$ over the Loess Plateau, used for normalization. This formulation preserves the structural information represented by *LAI* while moderately increasing the relative weight of vegetation in grid cells with stronger evapotranspiration. Accordingly, $LAI_{w}$ is intended as a diagnostic measure of vegetation conditions that are more closely associated with land–atmosphere moisture exchange than *LAI* alone.

It should be noted that LAIw is a derived indicator rather than a directly observed physical quantity. Its role in this study is therefore diagnostic rather than strictly mechanistic. The weighting does not imply that evapotranspiration is solely controlled by vegetation, nor that $LAI_{w}$ should be interpreted as an independent biophysical property. Instead, it is used to describe vegetation conditions under which structural canopy effects and evaporative activity jointly influence the likelihood of moisture returning to the study region as recycled precipitation.

At the grid scale, a multiple linear regression was then applied to estimate the vegetation-associated component of recycled precipitation over the Loess Plateau:

$$P_{rec} = d + a \cdot LAI_{w} + b \cdot T + c \cdot ssr \tag{6}$$

where $P_{rec}$ represents the grid-based recycled precipitation, defined as the amount of precipitation over the Loess Plateau originating from evaporation at a given grid cell and returning to the plateau through atmospheric moisture transport. $T$ and $ssr$ denote near-surface air temperature and surface shortwave radiation, which are included to account for major thermodynamic controls on moisture recycling. The coefficient $a$ represents the statistical sensitivity of recycled precipitation to $LAI_{w}$, conditional on $T$ and $ssr$.

Based on the estimated coefficient $a$, the vegetation-associated contribution to recycled precipitation is defined as:

$$P_{0} = a \cdot LAI_{w} \tag{7}$$

https://doi.org/10.5194/egusphere-2026-2206
Preprint. Discussion started: 4 May 2026


where $P_0$ represents the component of recycled precipitation statistically associated with vegetation conditions as characterized by $LAI_w$. Here, $P_0$ should be interpreted as a vegetation-associated diagnostic term rather than as a strictly causal estimate derived from process-based perturbation experiments. This term is subsequently used to construct precipitation scenarios with the vegetation-associated recycling effect removed.

The use of $LAI_w$ instead of the original $LAI$ is intended to better capture the joint role of vegetation structure and evapotranspiration intensity in regulating recycled precipitation during the peak growing season. However, to avoid over-interpreting the weighting scheme, the robustness of this diagnostic formulation was further evaluated by repeating the key analytical steps using unweighted $LAI$ as an alternative vegetation predictor. This comparison was used to assess whether the major results depend strongly on the specific construction of $LAI_w$, or whether they primarily reflect the broader vegetation pattern itself.

#### 2.3.3 Budyko–RF framework for assessing hydrological impacts of vegetation-associated precipitation recycling

The Budyko framework was originally developed for long-term water balance analysis, but recent advances have extended its application to sub-annual timescales by incorporating dynamic storage effects and time-varying parameters (Yang et al., 2026; Liu et al., 2025). At the monthly scale, explicitly accounting for soil water storage change can substantially improve the performance of Budyko-type equations, thereby supporting the feasibility of such approaches beyond traditional annual mean applications (Yang et al., 2026).

In this study, the Budyko framework is applied as a comparative diagnostic tool for the peak growing season (July–August), rather than as a strict representation of the full seasonal or annual water balance. The framework is used to isolate the first-order hydrological effects of vegetation-associated precipitation recycling under consistent land surface and atmospheric conditions. This seasonal application is conceptually consistent with previous monthly Budyko studies that emphasize the importance of parameter variability under changing hydroclimatic conditions (Chen et al., 2013).

To better represent sub-annual variability in land-surface and hydroclimatic conditions, the key Budyko parameter $n$ was allowed to vary across grid cells and years through a Random Forest (RF) model (Breiman, 2001). This treatment is conceptually consistent with previous monthly Budyko studies that emphasize the importance of storage effects and parameter variability under changing hydroclimatic and land-surface conditions. By linking $n$ to vegetation, soil moisture, and meteorological conditions, this Budyko–RF framework was used to evaluate the hydrological implications of vegetation-associated precipitation recycling.

Actual evapotranspiration ($E$) simulated by the Budyko framework was calculated using the Mezentsev–Choudhury–Yang equation:

$$E = \frac{ET_0 \cdot P}{(P^n + ET_0^n)^{1/n}} \tag{8}$$

where $P$ is precipitation, $ET_0$ is potential evapotranspiration, and $n$ is a dimensionless parameter characterizing integrated land surface properties.

https://doi.org/10.5194/egusphere-2026-2206
Preprint. Discussion started: 4 May 2026


Because $n$ is affected by vegetation conditions, soil water status, and atmospheric forcing, an RF regression model was used to estimate $n$ for each grid cell:

$$n = RF(VC, swvl1, swvl2, swvl3, swvl4, u, v, T, src, ssr) \quad (9)$$

where *VC* is vegetation cover; *swvl*1–*swvl*4 represent soil moisture in four layers; *u* and *v* are wind components; *T* is near-surface air temperature; *src* is surface runoff; and *ssr* is surface shortwave radiation.

To evaluate the performance of the Budyko–RF framework at the analysis scale used in this study, a two-step validation was performed. First, 80% of the samples were used for model training and the remaining 20% for testing. The RF model showed good predictive skill for $n$ in the test set (Fig. 2b, $R^2$=0.82), indicating that the effective Budyko parameter can be reasonably estimated from vegetation, hydrological, and meteorological predictors. Second, evapotranspiration estimated by the Budyko–RF framework was compared with observed evapotranspiration at the grid scale. The comparison showed strong agreement (Fig. 2c, $R^2$= 0.93), suggesting that the framework can satisfactorily reproduce actual evapotranspiration during the study period.

To further quantify the hydrological impacts of vegetation-associated precipitation recycling, a counterfactual precipitation scenario was constructed by removing the vegetation-associated recycled component from regional mean precipitation while keeping other climatic controls unchanged. For each year t, the study domain contains $N_t$ valid grid cells, and regional mean precipitation and potential evapotranspiration are denoted by $\bar{P}_t$ and $\overline{ET}_{0t}$, respectively. Based on the grid-scale vegetation-associated recycled precipitation $P_{0,i,t}$, the total contribution associated with a given set of grid cells $S$ is expressed as:

$$P_{0,t}^{(S)} = \sum_{i \in S} P_{0,i,t} \quad (10)$$

The precipitation scenario without vegetation-associated recycling is then defined at the regional mean scale as:

$$P_{\mathrm{clim},t}^{(S)} = \bar{P}_t - \frac{P_{0,t}^{(S)}}{N_t} \quad (11)$$

This formulation represents the removal of vegetation-associated recycling component as a uniform perturbation to regional mean precipitation, allowing direct comparison among years and among vegetation subsets.

Hydrological responses to the counterfactual precipitation were evaluated within the Budyko framework. For each year t, the Budyko parameter $n_t$ was held constant when comparing the baseline and counterfactual scenarios, so that changes in evapotranspiration can be attributed solely to differences in precipitation. Accordingly, regional mean evapotranspiration under baseline and counterfactual conditions is given by:

$$\bar{E}_t = \beta(\bar{P}_t, \overline{ET}_{0t}, n_t), \quad E_{\mathrm{clim},t}^{(S)} = \beta\left(P_{\mathrm{clim},t}^{(S)}, \overline{ET}_{0t}, n_t\right) \quad (12)$$

where $\beta(\cdot)$ denotes the Budyko mapping.

The vegetation-associated component of regional evapotranspiration associated with precipitation recycling is quantified by scenario differencing:

$$E_{0,t}^{(S)} = \bar{E}_t - E_{\mathrm{clim},t}^{(S)} \quad (13)$$

https://doi.org/10.5194/egusphere-2026-2206
Preprint. Discussion started: 4 May 2026


Regional aridity index is introduced to further characterize the regional hydroclimatic conditions, defined as:

$$AI_t = \frac{\bar{P}_t}{\bar{E}_t} \tag{14}$$

Here, AI is used as a diagnostic hydroclimatic index defined as $P/E$, rather than the conventional PET-based aridity index.

Regional surface water availability is defined as the difference between precipitation and evapotranspiration:

$$SWA_t = \bar{P}_t - \bar{E}_t \tag{15}$$

with the corresponding value under the counterfactual precipitation scenario given by:

$$SWA^{(S)}_{\mathrm{clim},t} = P^{(S)}_{\mathrm{clim},t} - E^{(S)}_{\mathrm{clim},t} \tag{16}$$

The relative contribution of vegetation-associated precipitation recycling to regional surface water availability is finally expressed as:

$$C^{(S)}_{SWA,t} = \frac{SWA_t - SWA^{(S)}_{\mathrm{clim},t}}{SWA_t} \times 100\% \tag{17}$$

This framework provides a consistent attribution of vegetation-associated precipitation recycling effects on regional evapotranspiration and surface water availability, and can be applied uniformly to the entire study domain as well as to vegetation subsets defined by $LAI_w$ magnitude or long-term $LAI_w$ trends.

## 3 Results

### 3.1 Spatiotemporal characteristics and sources of recycled precipitation over the Loess Plateau

Atmospheric moisture tracking based on WAM-2layers for the peak growing season (July–August) during 2000–2022 shows that precipitation over the Loess Plateau (LP) is sustained by both external moisture advection and internal moisture recycling. The mean amount of precipitation originating from evaporation at individual grid cells and returning to the LP ($P_{v0}$) is 2.05 mm, indicating that terrestrial evaporation contributes measurably to regional precipitation. The dominant moisture transport pathways supplying precipitation to the LP exhibit a clear bimodal pattern (Fig. 3a). One pathway is associated with the mid-latitude westerlies, through which moisture from Central and Western Asia is transported eastward toward the LP. The other is related to southerly transport driven by the southwest and southeast monsoons, which carries moisture from the Indian and Pacific Oceans northward into the study region.

Quantitative source attribution further shows that land-sourced moisture dominates the precipitation supply to the LP. On average, terrestrial moisture contributes approximately 71.0 mm of precipitation, accounting for 86.5% of total growing-season precipitation, whereas oceanic moisture contributes about 11.1 mm, corresponding to 13.5% (Fig. 3b). In terms of recycling pathways, externally advected precipitation accounts for 70.3 mm (85.6%), while internally recycled precipitation contributes 11.8 mm, representing 14.4% of total precipitation over the LP. During the study period, internally recycled precipitation

https://doi.org/10.5194/egusphere-2026-2206
Preprint. Discussion started: 4 May 2026


shows a declining trend of −0.073 mm yr⁻¹ (Fig. 3c). This result indicates a gradual weakening of the contribution of internal moisture recycling to growing-season precipitation over the LP.

**Figure. 3: Recycled precipitation over the Loess Plateau during the growing season (July–August, 2000–2022). (a) Spatial distribution of mean recycled precipitation and moisture transport. (b) Contributions of oceanic and terrestrial moisture sources and the partitioning between external and internal recycling. (c) Interannual variation of internally recycled precipitation.**

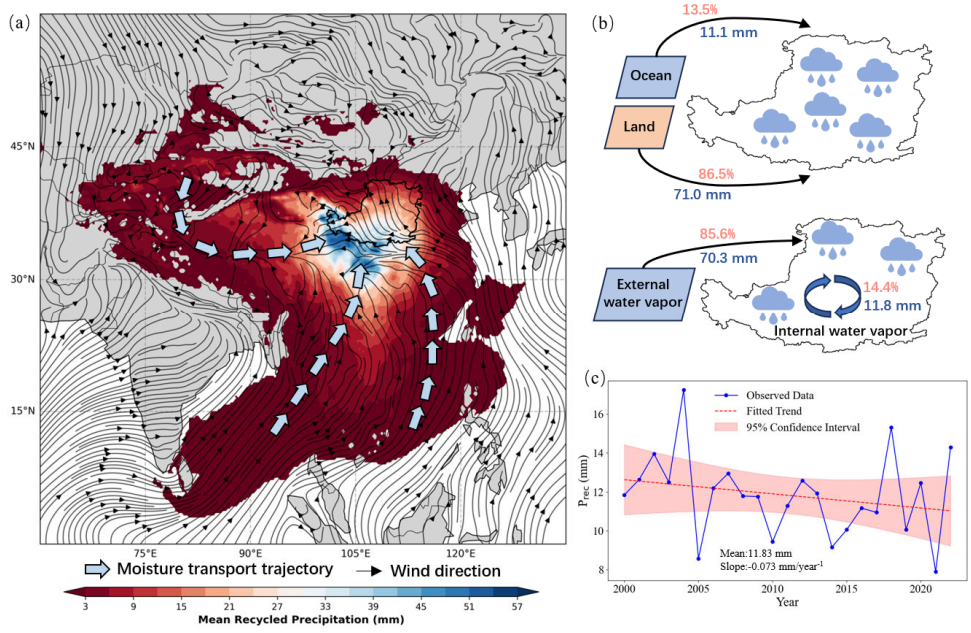


### 3.2 Vegetation-weighted patterns and contributions to recycled precipitation

To characterize the spatial patterns of vegetation conditions relevant to moisture recycling over the Loess Plateau, the vegetation-weighted index $LAI_w$ was analyzed at the grid scale. The spatial distribution and temporal trends of $LAI_w$ are shown in Fig. 4a–b. The multi-year mean $LAI_w$ over the Loess Plateau is 0.45, and approximately 90.6% of grid cells exhibit $LAI_w$ values lower than 1, mainly in the northwestern part of the plateau where vegetation cover is relatively sparse. In contrast, grid cells with $LAI_w$ values greater than 4 account for only 2.9% of the region and are concentrated in localized areas of the southeastern Loess Plateau. At the regional scale, 48.7% of grid cells show increasing trends in $LAI_w$, whereas 26.5% show decreasing trends. Spatially, increases in $LAI_w$ are mainly located in areas that already exhibit relatively high $LAI_w$ values (Fig. 4b).

To further evaluate the statistical association between vegetation conditions and recycled precipitation, a grid-based multiple linear regression was performed with recycled precipitation ($P_{rec}$) as the dependent variable and $LAI_w$, near-surface air temperature, and surface shortwave radiation as explanatory variables. Here, $P_{rec}$ represents the amount of precipitation over

https://doi.org/10.5194/egusphere-2026-2206
Preprint. Discussion started: 4 May 2026


the Loess Plateau that originates from evaporation at a given grid cell and subsequently returns to the plateau through atmospheric moisture transport. The regional mean of the sensitivity coefficient of $LAI_w$ ($a$) is 2.34, and 57.5% of grid cells exhibit positive $a$ values, indicating that higher $LAI_w$ is statistically associated with greater recycled precipitation across much of the study area (Fig. 4c–d).

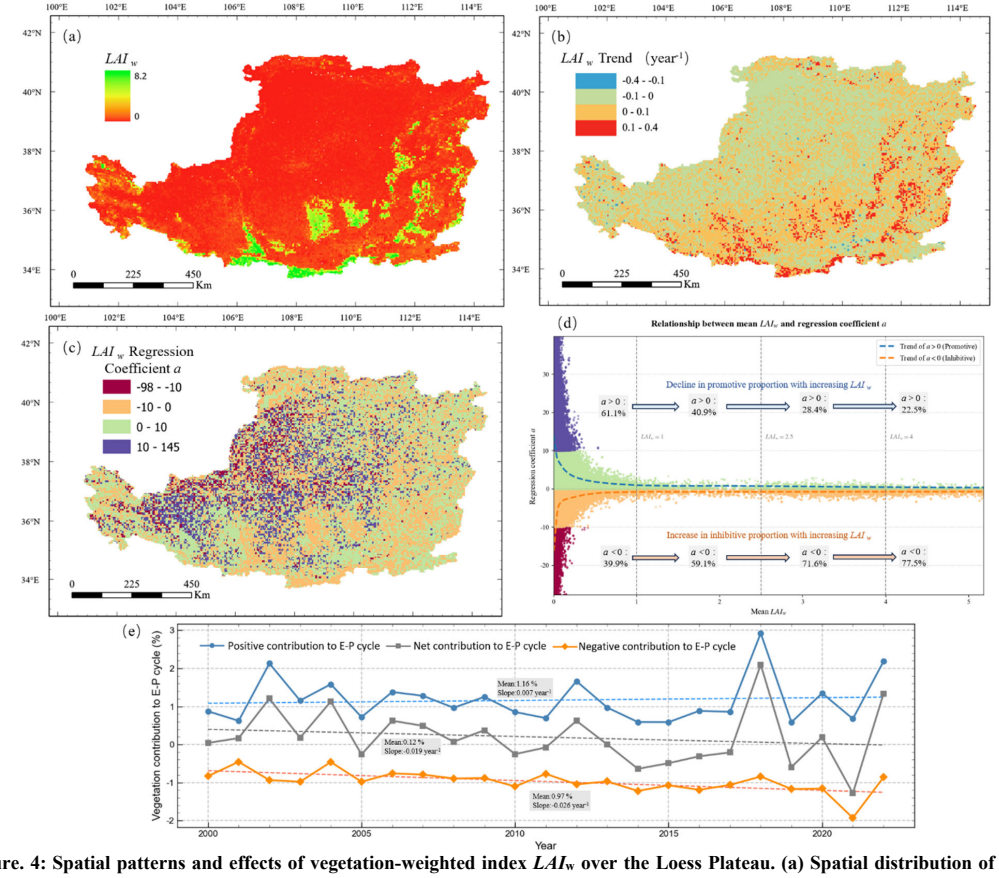


**Figure. 4: Spatial patterns and effects of vegetation-weighted index $LAI_w$ over the Loess Plateau. (a) Spatial distribution of mean $LAI_w$ during the growing season. (b) Spatial patterns of linear trends in $LAI_w$. (c) Spatial distribution of the regression coefficient a. (d) Relationship between mean $LAI_w$ and the regression coefficient a. (e) Interannual variation of vegetation contributions to the evaporation–precipitation cycle.**

Fig. 4e shows the interannual evolution of the vegetation-associated contribution to the evaporation–precipitation (E–P) cycle, decomposed into positive, negative, and net components. Over the study period, the mean positive contribution is 1.16%, with a weak increasing trend of 0.007% $yr^{-1}$. In contrast, the mean negative contribution is −0.97%, with a decreasing trend of

https://doi.org/10.5194/egusphere-2026-2206
Preprint. Discussion started: 4 May 2026


−0.026% $yr^{-1}$. As a combined result of these opposing components, the net vegetation-associated contribution to the E–P cycle remains small, with a mean value of 0.12% and a slight negative trend of −0.019% $yr^{-1}$. Overall, these results show that positive and negative vegetation-associated influences on internal moisture recycling largely offset each other at the regional scale.

### 3.3 Declining surface water availability and hydrological implications of vegetation-associated precipitation recycling

A pronounced drying tendency is observed over the Loess Plateau during the growing season from 2000 to 2022 (Fig. 5a). Interannual variations in precipitation (*P*), evapotranspiration (*E*), surface water availability (*SWA*), and the aridity index (*AI*) show that regional precipitation exhibits a non-significant declining trend of −0.0043 mm $yr^{-1}$, whereas evapotranspiration shows a significant increasing trend of 0.31 mm $yr^{-1}$. The contrasting changes in precipitation and evapotranspiration correspond to increasingly dry hydroclimatic conditions over the study period. Although the interannual variations in *SWA* and *AI* generally follow the temporal pattern of precipitation, both indices exhibit significant downward trends under increasing evapotranspiration, with *SWA* decreasing at a rate of −0.34 mm $yr^{-1}$ and *AI* decreasing at a rate of −0.008 $yr^{-1}$.

The spatial distribution of mean *SWA* and its temporal trends also shows clear heterogeneity across the Loess Plateau (Fig. 5b–c). Higher *SWA* values are mainly distributed in the southeastern part of the region, whereas persistently low *SWA* values characterize the northwestern arid areas. Declining SWA trends occur in both relatively high-SWA and low-SWA regions, whereas increasing trends are mainly concentrated in the southwestern Loess Plateau. Although 51% of grid cells show increasing trends in *SWA* and 49% show decreasing trends, the pattern becomes asymmetric when statistical significance is considered. Among the 56.6% of grid cells with significant *SWA* trends ($P < 0.05$), 40% exhibit significant declines, whereas only 16.6% show significant increases. This indicates that the most robust regional signal is a widespread decline in *SWA*.

https://doi.org/10.5194/egusphere-2026-2206
Preprint. Discussion started: 4 May 2026


To quantify the hydrological implications of vegetation-associated recycled precipitation ($P_0$), the $P_0$ term estimated in Section 3.2 was subtracted from total precipitation and the resulting water-balance components were evaluated within the Budyko–RF framework. The results (Fig. 5d) show that the mean relative contributions of vegetation-associated recycled precipitation to *P*, *E*, and *SWA* are 0.059%, 0.02%, and 0.107%, respectively. A consistent response pattern is observed across the study region: grid cells with positive $P_0$ contributions to precipitation also show higher *E* and *SWA*, whereas negative $P_0$ contributions are accompanied by concurrent reductions in both *E* and *SWA*. Overall, the positive hydrological contribution of *P*0 is relatively more evident in drier areas with lower *SWA*.

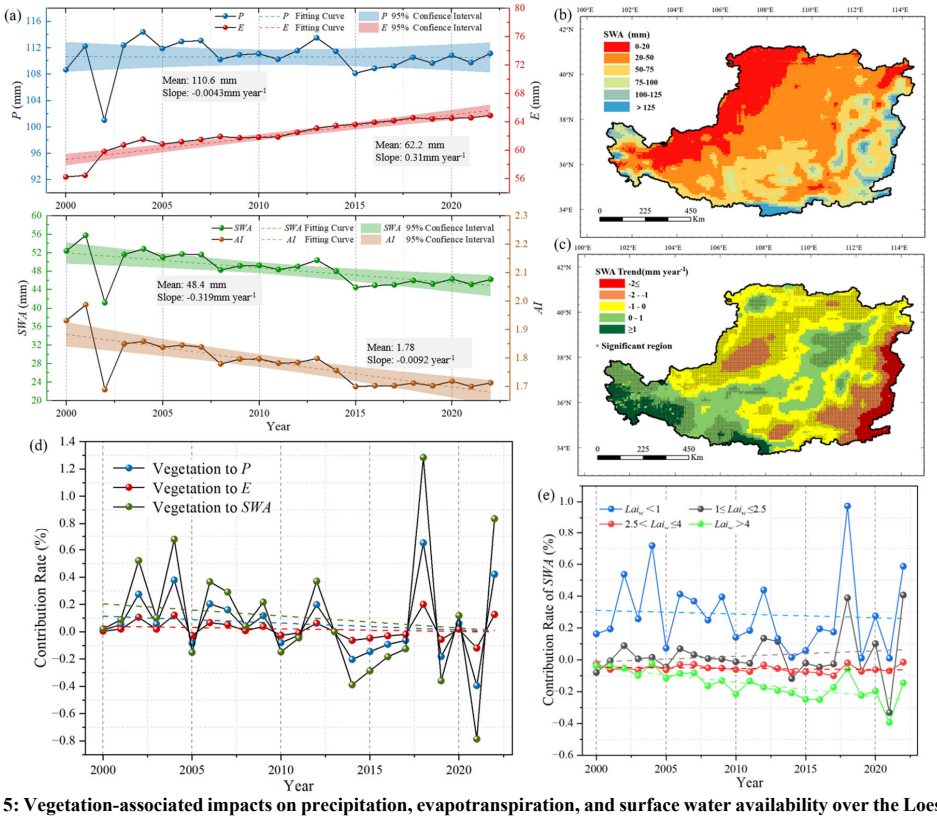


**Figure. 5: Vegetation-associated impacts on precipitation, evapotranspiration, and surface water availability over the Loess Plateau. (a) Interannual variations of growing-season *P*, *E*, *SWA*. and *AI*. (b) Spatial distribution of *SWA*. (c) Spatial patterns of *SWA*. trends. (d) Interannual contribution rates of vegetation to *P*, *E*, and *SWA*. (e) Contribution rates of vegetation to *SWA*. under different $LAI_w$ classes.**

Fig. 5e further shows a systematic dependence of the *SWA* contribution associated with vegetation-related recycled precipitation on $LAI_w$. Under low-$LAI_w$ conditions ($LAI_w < 1$), the contribution to *SWA* remains consistently positive, with a

https://doi.org/10.5194/egusphere-2026-2206
Preprint. Discussion started: 4 May 2026


mean value of 0.2855% and no negative values across all years, although it shows a weakening trend of −0.0023% $yr^{-1}$. As $LAI_w$ increases, this positive contribution diminishes and gradually shifts toward negative values. For intermediate $LAI_w$ conditions ($1 \leq LAI_w \leq 2.5$), the mean contribution is close to zero (0.02565%) and shows substantial interannual variability, with negative values occurring in 11 years; however, a modest positive trend (0.0035% $yr^{-1}$) is still observed. In contrast, high-$LAI_w$ conditions ($LAI_w \geq 2.5$) are characterized by persistently negative contributions to *SWA*, with mean values of −0.0361% for $2.5 \leq LAI_w \leq 4$ and −0.1495% for $LAI_w > 4$, and the strongest negative trend (−0.0092% $yr^{-1}$) occurring in the highest-$LAI_w$ class. Overall, these results indicate a systematic shift from weakly positive to increasingly negative *SWA* contributions along the $LAI_w$ gradient.

## 4 Discussion

### 4.1 Hydroclimatic constraints and precipitation recycling over the Loess Plateau

Recent global assessments have shown that surface water availability (*SWA*) has increased over large parts of the terrestrial surface, mainly because precipitation has increased faster than evapotranspiration across more than 53% of global land areas (Cui et al., 2022). In contrast, our results indicate a decline in *SWA* over the Loess Plateau during the study period (Fig. 5a). In this arid and semi-arid region, evapotranspiration increased faster than precipitation, leading to a reduction in available surface water. Similar drying trends have been widely reported in dryland regions, where climate warming is expected to increase drought frequency and severity (Stevenson et al., 2022; Tabari et al., 2021), and where regional water resources often decline under limited precipitation and enhanced evaporation (Lai et al., 2022). These results together suggest that water availability in arid and semi-arid systems remains strongly constrained by limited precipitation and high evaporative demand. Under this hydroclimatic setting, precipitation over the Loess Plateau still depends strongly on external moisture supply. The WAM-2layers results show that Central China is the dominant external moisture source for precipitation over the Loess Plateau (Fig. 3a). This pattern is broadly consistent with previous studies based on other moisture-tracking approaches, including FLEXPART-based analyses (Hu et al., 2018) and WAM-2layers simulations (Cao et al., 2024). This consistency suggests that the large-scale circulation pattern controlling moisture transport to the region is relatively stable.

Within this externally constrained background, internal precipitation recycling contributed about 14.4% of total precipitation over the Loess Plateau during the study period (Fig. 3b–c). This estimate is higher than values reported in some previous studies, such as 7% from the UTrack Lagrangian moisture-tracking model (Wang, Liu et al., 2023) and 9.16 ± 0.35% to 10.18 ± 0.28% from the Dynamic Precipitation Recycling Method (Tian et al., 2022). One likely reason is the seasonal focus of this study. Our analysis is limited to July and August, when vegetation activity, evapotranspiration, and land–atmosphere coupling are strongest over the Loess Plateau (Li et al., 2024; Guo et al., 2025). During this period, land-derived moisture accounts for about 86.5% of the total precipitation supply (Fig. 3b). Stronger transpiration and soil evaporation may therefore increase the fraction of precipitation recycled from regional land surfaces. In this sense, the relatively high internal recycling ratio reported

https://doi.org/10.5194/egusphere-2026-2206
Preprint. Discussion started: 4 May 2026


here is more likely to reflect seasonal amplification during the peak growing season than a uniformly high contribution throughout the year.

### 4.2 Conditional and nonlinear vegetation-associated effects on surface water availability

Under water-limited conditions, vegetation influences regional water cycling through two competing pathways. On the one hand, enhanced vegetation activity increases evapotranspiration and strengthens land–atmosphere coupling, which may promote the return of locally evaporated moisture as precipitation (Sterling et al., 2013). On the other hand, vegetation growth also increases terrestrial water consumption, which can reduce soil moisture and limit the water available for surface and subsurface hydrological processes (Piao et al., 2020). The coexistence of these two pathways helps explain why vegetation-associated effects on internal moisture recycling do not lead to a uniformly positive effect on surface water availability.

At the regional scale, the long-term vegetation-associated influence on the evaporation–precipitation cycle appears to largely cancel out in net effect. Vegetation-related moisture recycling can enhance precipitation during periods of active growth, but this effect is accompanied by an increase in evapotranspiration. As a result, the net contribution to regional water availability remains very small (Fig. 4e; Fig. 5d). This small net effect should be interpreted in the context of the process boundary considered here. Specifically, this study quantifies only the vegetation-associated contribution to precipitation generated from evaporation within the Loess Plateau and recycled back to the plateau itself, whereas internally recycled precipitation accounts for only 14.4% of total growing-season precipitation (Fig. 3c). Consequently, even a measurable vegetation effect on this internally recycled component becomes substantially diluted when expressed relative to total precipitation and, therefore, total surface water availability. In addition, the regional mean signal reflects strong compensation between positive and negative vegetation-associated effects. The strongest positive and negative effects correspond to 12.2% and −32.2% of the internally recycled precipitation component, respectively (Fig. 3c; Fig. 6a). Therefore, the low net value arises not only from the limited share of internal recycling in the total precipitation supply, but also from substantial cancellation between opposing responses across vegetation conditions. This small net effect does not imply that vegetation–atmosphere feedbacks are negligible. Rather, it indicates that under the dry background conditions of the Loess Plateau, the additional precipitation returned through recycling is generally too limited to compensate for the additional water consumption associated with vegetation growth. Therefore, the main implication of our results is not that vegetation substantially increases available water, but that the hydrological benefit of vegetation-related recycling is strongly constrained by background hydroclimatic conditions. This contrasts with humid or energy-limited regions, where vegetation-associated moisture recycling can more readily translate into effective water gains (Cui et al., 2022; Meier et al., 2021). The comparison further highlights the importance of climatic context in shaping vegetation–water interactions.

https://doi.org/10.5194/egusphere-2026-2206
Preprint. Discussion started: 4 May 2026


More importantly, the influence of vegetation on surface water availability shows a clear nonlinear pattern along the $LAI_w$ gradient. Two results support this interpretation. First, the contribution of vegetation-associated recycled precipitation to *SWA* shifts from positive under low-$LAI_w$ conditions to negative under high-$LAI_w$ conditions. This suggests that the hydrological benefit of moisture recycling is mainly confined to relatively sparse vegetation cover and weakens once vegetation density increases beyond a moderate level (Fig. 5e; Fig. 6a). Second, the temporal evolution of the positive and negative components shows an asymmetric compensation pattern. Positive contributions remain small and intermittent, whereas negative contributions become more persistent with increasing $LAI_w$ (Fig. 4e; Fig. 5e; Fig. 6b). This pattern is consistent with the limited water storage capacity and strong evaporative sensitivity of the Loess Plateau. Under such conditions, further vegetation growth is more likely to intensify water consumption than to generate sustained increases in surface water availability. The scientific value of the small regional mean effect therefore lies less in its magnitude than in what it reveals about the hydrological conditions under which vegetation-related precipitation recycling shifts from weakly beneficial to persistently adverse.

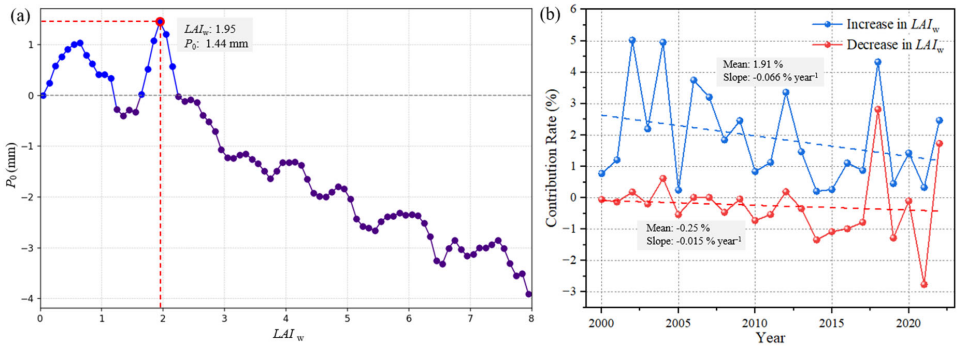


**Figure. 6: Vegetation-related variations in recycled precipitation and surface water availability: (a) recycled precipitation along the $LAI_w$ gradient, (b) Contribution rates of vegetation to *SWA* under increasing and decreasing $LAI_w$ conditions.**

### 4.3 Robustness of the LAIw diagnostic framework

Because $LAI_w$ is a derived diagnostic indicator rather than a directly observed physical variable, its formulation may raise the question of whether the identified hydrological patterns depend strongly on the weighting scheme itself. In particular, weighting *LAI* by normalized actual evapotranspiration could, in principle, enhance the apparent association with recycled precipitation and thereby affect the inferred threshold-like behavior. To test this possibility, we repeated the full analytical workflow using the original, unweighted peak-growing-season *LAI* in place of $LAI_w$. This parallel analysis included both the multiple linear regression for $P_{rec}$ and the subsequent Budyko-based attribution of hydrological effects. The resulting vegetation-associated contributions to surface water availability ($C_{SWA}$) were then compared between the *LAI*-based and $LAI_w$-based frameworks at the regional mean scale and across the four vegetation classes defined in Section 3.3.

https://doi.org/10.5194/egusphere-2026-2206
Preprint. Discussion started: 4 May 2026


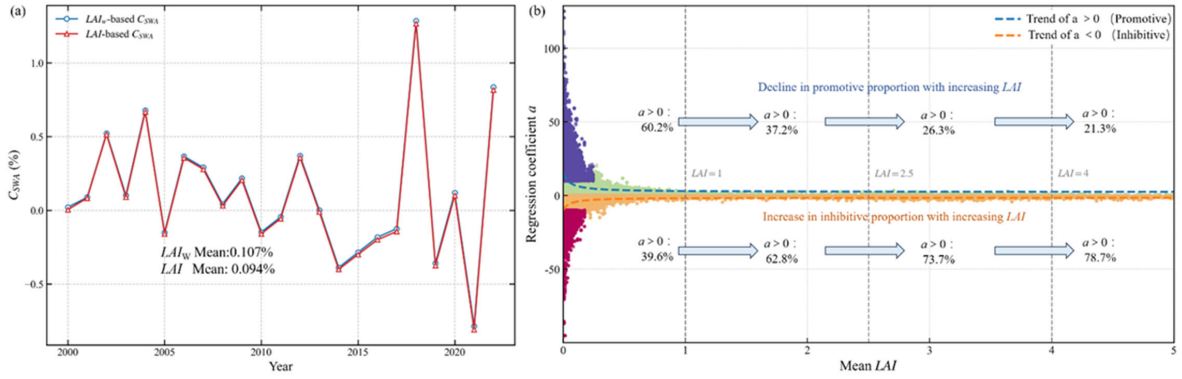


**Figure. 7: Vegetation-related variations in surface water availability and vegetation contribution under *LAI* and $LAI_w$ conditions: (a) interannual variations in vegetation-related $C_{SWA}$ estimated from *LAI* and $LAI_w$, (b) contribution rates of vegetation to *SWA* under promotive and inhibitive conditions along the mean *LAI* gradient.**

The comparison shows that the major results are highly robust to this substitution. At the regional mean scale, the interannual variations in $P_0$ and $C_{SWA}$ derived from the two frameworks are nearly identical, with Pearson correlation coefficients of 0.99996 and 0.99995, respectively (Fig. 7). Their multi-year mean values are likewise very close. For example, the mean $C_{SWA}$ is 0.107% in the $LAI_w$-based framework and 0.094% in the *LAI*-based framework, with a mean absolute difference of only 0.013 percentage points. This close agreement suggests that the threshold-like hydrological response identified in this study is not an artifact of the $LAI_w$ formulation. Rather, $LAI_w$ mainly acts as a diagnostic rescaling of the original *LAI* pattern, while the dominant signal appears to be rooted in the underlying vegetation gradient itself. In this sense, the use of $LAI_w$ does not change the qualitative conclusions, but instead provides a slightly more process-oriented representation of vegetation conditions under different evaporative backgrounds.

### 4.4 Limitations and Research Prospects

This study provides a quantitative assessment of vegetation-associated precipitation recycling and its contribution to surface water availability during the peak growing season over the Loess Plateau, but several limitations should be noted.

First, the seasonal focus of this study should be explicitly acknowledged. By concentrating on July and August, the analysis targets the period when vegetation activity and land–atmosphere coupling are strongest over the Loess Plateau, but it does not represent the full growing season (June–September) or annual water balance. This seasonal restriction is methodologically necessitated by the WAM-2layers tracking configuration, which requires computational trade-offs between temporal coverage and process resolution. The two-month focus captures the peak of vegetation-precipitation recycling interactions but excludes the early growing season (June) when vegetation is still developing and late season (September) when soil moisture depletion may limit evapotranspiration. Consequently, the results should be interpreted as reflecting vegetation-associated hydrological effects during the period of maximum coupling intensity, rather than as representative of the entire growing season. Future

https://doi.org/10.5194/egusphere-2026-2206
Preprint. Discussion started: 4 May 2026


work should extend this framework across the full growing season to test the robustness of the threshold-like behavior identified here.

Second, the analysis focuses on hydroclimatic responses within the Loess Plateau itself. It does not explicitly consider the possible effects of vegetation-related moisture export on downwind regions, nor does it examine how changes in external source areas may influence local precipitation and water availability. Vegetation-enhanced evapotranspiration may reduce local water availability while also contributing to precipitation elsewhere through atmospheric moisture transport (Greve et al., 2025). A more complete evaluation would therefore require an integrated local–downwind framework. In this sense, the present results should be interpreted as reflecting the local hydrological consequences of vegetation-associated recycling within the Loess Plateau, rather than the full hydroclimatic footprint of vegetation-induced moisture redistribution.

Third, uncertainty arises from both the input datasets and the attribution framework. Recycled precipitation and hydrological responses were estimated using multiple reanalysis and remote-sensing datasets, and uncertainties in these products may propagate through both the moisture-tracking and Budyko–RF analyses. In addition, $LAI_w$ is a diagnostic indicator rather than a directly observed physical variable, and the P0 term reflects a statistical attribution of vegetation-associated recycled precipitation rather than a strictly causal estimate from process-based perturbation experiments. The counterfactual analysis therefore isolates a first-order hydrological effect, but does not resolve secondary feedbacks associated with soil moisture, vegetation adjustment, or atmospheric circulation.

## 5 Conclusions

The Loess Plateau is a water-limited region in arid and semi-arid northern China, where large-scale vegetation restoration has raised an important question: can vegetation-related precipitation recycling meaningfully alleviate regional water scarcity? To address this question, this study combined an Eulerian atmospheric moisture-tracking model with a random forest–enhanced Budyko framework to examine peak growing season water cycling over the Loess Plateau during July and August from 2000 to 2022, the period when vegetation–atmosphere coupling is expected to be strongest.

The results show that growing-season precipitation over the Loess Plateau is dominated by land-derived moisture. Terrestrial evaporation contributes 86.5% of total precipitation, while oceanic sources contribute 13.5%. Internal moisture recycling contributes 11.83 mm on average, accounting for 14.4% of total precipitation, but shows a declining trend of −0.073 mm $yr^{-1}$ during the study period. Vegetation-related processes enhance land–atmosphere coupling, but their net contribution to the evaporation–precipitation cycle remains small, at about 0.12%, because positive effects of about 1.16% are largely offset by negative effects of about −0.97%.

During the same period, the Loess Plateau showed a clear drying tendency. Evapotranspiration increased at 0.31 mm $yr^{-1}$, while surface water availability decreased at −0.34 mm $yr^{-1}$. At the regional mean scale, the hydrological contribution of vegetation-associated recycled precipitation is limited. On average, it accounts for only 0.059% of precipitation and 0.107% of surface water availability. This small regional mean contribution partly reflects the fact that the analysis isolates only the

https://doi.org/10.5194/egusphere-2026-2206
Preprint. Discussion started: 4 May 2026


vegetation-associated component of internally recycled precipitation, which itself represents a limited fraction of total growing-season precipitation, and that positive and negative vegetation-associated effects partly offset each other. However, this small regional mean effect is not spatially uniform. Along the LAIw gradient, the contribution shows a threshold-like pattern. Under low-$LAI_w$ conditions ($LAI_w < 1$), vegetation-associated recycling contributes weakly but consistently positively to surface water availability, with a mean contribution of about 0.29%. Under high-$LAI_w$ conditions ($LAI_w \geq 2.5$), the contribution becomes persistently negative, with mean values reaching about −0.15% and tending to become more negative over time.

Overall, these results suggest that under the water-limited conditions of the Loess Plateau, stronger vegetation–atmosphere coupling does not necessarily lead to greater surface water availability. The additional precipitation returned through recycling is generally too small to offset the additional terrestrial water consumption associated with vegetation growth. The hydrological significance of vegetation-related precipitation recycling in this dryland region therefore appears to lie less in increasing mean water availability than in revealing the hydroclimatic conditions under which vegetation effects shift from weakly positive to persistently negative. More broadly, these findings suggest that the hydrological consequences of vegetation restoration in drylands need to be evaluated within the context of background climatic constraints, process boundaries, and vegetation thresholds. While these findings are specific to the peak growing season, they highlight the importance of evaluating vegetation restoration effects within the context of seasonal hydroclimatic constraints and vegetation density thresholds.

## Code and data availability

The ERA5 and ERA5-Land reanalysis data used in this study are publicly available from the European Centre for Medium-Range Weather Forecasts (ECMWF) Climate Data Store. The GLEAM v3.6a evapotranspiration data are publicly available from the GLEAM project. The HiQ-LAI dataset is publicly available via Zenodo, and the fractional vegetation cover dataset is available from the National Tibetan Plateau Data Center. The WAM-2layers model used for atmospheric moisture tracking is available from the corresponding published source. The code used for data processing, statistical analysis, and figure generation in this study is available from the corresponding author upon reasonable request.

## Supplement link

## Author contributions

Jiaxiang Deng conducted the formal analysis, processed the data, and prepared the original manuscript draft. Quan Quan conceived and designed the study, supervised the research, and revised the manuscript. Shuangcheng Tang contributed to the methodology, interpretation of the results, and manuscript revision. Hanbo Yang contributed to the methodology and

https://doi.org/10.5194/egusphere-2026-2206
Preprint. Discussion started: 4 May 2026


interpretation of the results. Xiaoyu Song contributed to data curation and manuscript revision. All authors discussed the results and approved the final manuscript.

**Competing interests**

The authors declare that they have no conflict of interest.

**Disclaimer**

Copernicus Publications remains neutral with regard to jurisdictional claims made in the text, published maps, institutional affiliations, or any other geographical representation in this paper. While Copernicus Publications makes every effort to include appropriate place names, the final responsibility lies with the authors. Views expressed in the text are those of the authors and do not necessarily reflect the views of the publisher.

**Acknowledgements**

The authors would like to express their gratitude to the National Key Research and Development Program of China for their financial support under Grant No. 2024YFF1306901.

**Financial support**

The authors would like to express their gratitude to the National Key Research and Development Program of China for their financial support under Grant No. 2024YFF1306901.

**Review statement**

The review statement will be added by Copernicus Publications listing the handling editor as well as all contributing referees according to their status anonymous or identified.

**References**

An, Q., Liu, L., Cheng, Y., Liu, J., Staal, A., Huang, G., 2025. Unraveling the role of moisture recycling in water consumption across different ecosystems in China. Journal of Hydrology 662, 134020. https://doi.org/10.1016/j.jhydrol.2025.134020

Budyko, M.I., 1974. Climate and life. Academic, San Diego, Calif.

https://doi.org/10.5194/egusphere-2026-2206
Preprint. Discussion started: 4 May 2026


555 Cao, M., Wang, W., Wei, J., Forzieri, G., Fetzer, I., Wang-Erlandsson, L., 2024. Revegetation impacts on moisture recycling and precipitation trends in the Chinese Loess Plateau. Water Resources Research 60, e2024WR038199. https://doi.org/10.1029/2024WR038199

Cui, J., Lian, X., Huntingford, C., Gimeno, L., Wang, T., Ding, J., He, M., Xu, H., Chen, A., Gentine, P., Piao, S., 2022. Global water availability boosted by vegetation-driven changes in atmospheric moisture transport. Nature Geoscience 15, 982-988. 560 https://doi.org/10.1038/s41561-022-01061-7

Deng, Y., Wang, S., Bai, X., Luo, G., Wu, L., Chen, F., Wang, J., Li, C., Yang, Y., Hu, Z., Tian, S., Lu, Q., 2020. Vegetation greening intensified soil drying in some semi-arid and arid areas of the world. Agricultural and Forest Meteorology 292-293, 108103. https://doi.org/10.1016/j.agrformet.2020.108103

Dominguez, F., Hu, H., Martinez, J.A., 2020. Two-layer dynamic recycling model (2L-DRM): Learning from moisture 565 tracking models of different complexity. Journal of Hydrometeorology 21, 3-16. https://doi.org/10.1175/JHM-D-19-0101.1

Feng, X., Fu, B., Piao, S., Wang, S., Ciais, P., Zeng, Z., Lü, Y., Zeng, Y., Li, Y., Jiang, X., Wu, B., 2016. Revegetation in China's Loess Plateau is approaching sustainable water resource limits. Nature Climate Change 6, 1019-1022. https://doi.org/10.1038/nclimate3092

Gao, J.X., S.Y., Zhang, H.W., Chen, X.H., Zhang, W.G., Shen, W.M., Xiao, T., Zhang, Y.H., 2024. China regional 250m 570 fractional vegetation cover data set (2000-2023). National Tibetan Plateau Data Center. https://doi.org/10.11888/Terre.tpdc.300330

Giorgi, F., Coppola, E., Raffaele, F., 2014. A consistent picture of the hydroclimatic response to global warming from multiple indices: Models and observations. Journal of Geophysical Research: Atmospheres 119, 11695-11708. https://doi.org/10.1002/2014JD022238

575 Greve, P., Schmitt, A.U., Miralles, D.G., McDermid, S., Findell, K.L., García-García, A., Peng, J., 2025. Observational evidence of increased afternoon rainfall downwind of irrigated areas. Nature Communications 16, 3415. https://doi.org/10.1038/s41467-025-58729-y

Guo, J., Fan, L., Feng, P., Sun, X., Xue, S., 2025. Response of vegetation evapotranspiration to landscape pattern changes in an arid region: A case study of the Loess Plateau, China. CATENA 252, 108878. https://doi.org/10.1016/j.catena.2025.108878

580 He, C., Liu, Z., Wu, J., Pan, X., Fang, Z., Li, J., Bryan, B.A., 2021. Future global urban water scarcity and potential solutions. Nature Communications 12, 4667. https://doi.org/10.1038/s41467-021-25026-3

He, Y., Tian, W., Huang, J., Wang, G., Ren, Y., Yan, H., Yu, H., Guan, X., Hu, H., 2021. The mechanism of increasing summer water vapor over the Tibetan Plateau. Journal of Geophysical Research: Atmospheres 126, e2020JD034166. https://doi.org/10.1029/2020JD034166

585 Hersbach, H., et al., 2020. The ERA5 global reanalysis. Quarterly Journal of the Royal Meteorological Society 146, 1999-2049. https://doi.org/10.1002/qj.3803

Hu, Q., Jiang, D., Lang, X., Xu, B., 2018. Moisture sources of the Chinese Loess Plateau during 1979-2009. Palaeogeography, Palaeoclimatology, Palaeoecology 509, 156-163. https://doi.org/10.1016/j.palaeo.2016.12.030

https://doi.org/10.5194/egusphere-2026-2206
Preprint. Discussion started: 4 May 2026


Huang, J., Li, Y., Fu, C., Chen, F., Fu, Q., Dai, A., Shinoda, M., Ma, Z., Guo, W., Li, Z., Zhang, L., Liu, Y., Yu, H., He, Y., Xie, Y., Guan, X., Ji, M., Lin, L., Wang, S., Wang, G., 2017. Dryland climate change: Recent progress and challenges: Dryland climate change. Reviews of Geophysics 55. https://doi.org/10.1002/2016RG000550

Huang, J., Yu, H., Guan, X., Wang, G., Guo, R., 2016. Accelerated dryland expansion under climate change. Nature Climate Change 6, 166-171. https://doi.org/10.1038/nclimate2837

Jiao, D., Xu, N., Yang, F., Xu, K., 2021. Evaluation of spatial-temporal variation performance of ERA5 precipitation data in China. Scientific Reports 11, 17956. https://doi.org/10.1038/s41598-021-97432-y

Kalverla, P., Benedict, I., Weijenborg, C., van der Ent, R.J., 2025. Atmospheric moisture tracking with WAM2layers v3. Geoscientific Model Development 18, 4335-4352. https://doi.org/10.5194/gmd-18-4335-2025

Kummu, M., Guillaume, J.H.A., de Moel, H., Eisner, S., Flörke, M., Porkka, M., Siebert, S., Veldkamp, T.I.E., Ward, P.J., 2016. The world's road to water scarcity: shortage and stress in the 20th century and pathways towards sustainability. Scientific Reports 6, 38495. https://doi.org/10.1038/srep38495

Lai, J., Li, Y., Chen, J., Niu, G.-Y., Lin, P., Li, Q., Wang, L., Han, J., Luo, Z., Sun, Y., 2022. Massive crop expansion threatens agriculture and water sustainability in northwestern China. Environmental Research Letters 17, 034003. https://doi.org/10.1088/1748-9326/ac46e8

Li, C., Fu, B., Wang, S., Stringer, L.C., Wang, Y., Li, Z., Liu, Y., Zhou, W., 2021. Drivers and impacts of changes in China's drylands. Nature Reviews Earth & Environment 2, 858-873. https://doi.org/10.1038/s43017-021-00226-z

Li, R., Fan, B., Jin, Z., Hao, M., Liu, H., Zhang, Y., Jiang, Y., Yao, H., Lin, K., Guo, L., 2024. Divergent rainfall infiltration patterns on the Chinese Loess Plateau between growing and non-growing seasons after long-term revegetation. Journal of Hydrology 641, 131816. https://doi.org/10.1016/j.jhydrol.2024.131816

Li, Z., Wang, S., Li, C., Ye, C., Gao, D., Chen, P., 2022. The trend shift caused by ecological restoration accelerates the vegetation greening of China's drylands since the 1980s. Environmental Research Letters 17(4), 044062. https://doi.org/10.1088/1748-9326/ac55b8

Liu, R., Yang, L., Shi, Z., Xing, M., 2025. Assessment of the applicability of multi-satellite precipitation products on the Loess Plateau over the past four decades. International Journal of Applied Earth Observation and Geoinformation 141, 104634. https://doi.org/10.1016/j.jag.2025.104634

Liu, W., Liu, P., Cheng, L., Zhang, X., Zhou, L., 2025. Identification of time-varying parameters of a monthly Budyko function in US MOPEX catchments and its implications. Journal of Hydrology: Regional Studies 59, 102348. https://doi.org/10.1016/j.ejrh.2025.102348

Martens, B., Miralles, D.G., Lievens, H., van der Schalie, R., de Jeu, R.A.M., Fernández-Prieto, D., Beck, H.E., Dorigo, W.A., Verhoest, N.E.C., 2017. GLEAM v3: satellite-based land evaporation and root-zone soil moisture. Geoscientific Model Development 10, 1903-1925. https://doi.org/10.5194/gmd-10-1903-2017

Meier, R., Schwaab, J., Seneviratne, S.I., Sprenger, M., Lewis, E., Davin, E.L., 2021. Empirical estimate of forestation-induced precipitation changes in Europe. Nature Geoscience 14, 473-478. https://doi.org/10.1038/s41561-021-00773-6

https://doi.org/10.5194/egusphere-2026-2206
Preprint. Discussion started: 4 May 2026


Piao, S., Wang, X., Park, T., Chen, C., Lian, X., He, Y., Bjerke, J.W., Chen, A., Ciais, P., Tømmervik, H., Nemani, R.R., Myneni, R.B., 2020. Characteristics, drivers and feedbacks of global greening. Nature Reviews Earth & Environment 1, 14-27. https://doi.org/10.1038/s43017-019-0001-x

Sterling, S.M., Ducharne, A., Polcher, J., 2013. The impact of global land-cover change on the terrestrial water cycle. Nature Climate Change 3, 385-390. https://doi.org/10.1038/nclimate1690

Stevenson, S., Coats, S., Touma, D., Cole, J., Lehner, F., Fasullo, J., Otto-Bliesner, B., 2022. Twenty-first century hydroclimate: A continually changing baseline, with more frequent extremes. Proceedings of the National Academy of Sciences 119, e2108124119. https://doi.org/10.1073/pnas.2108124119

Tabari, H., Hosseinzadehtalaei, P., Thiery, W., Willems, P., 2021. Amplified drought and flood risk under future socioeconomic and climatic change. Earth's Future 9, e2021EF002295. https://doi.org/10.1029/2021EF002295

Te Wierik, S.A., Keune, J., Miralles, D.G., et al., 2022. The contribution of transpiration to precipitation over African watersheds. Water Resources Research 58(11), e2021WR031721. https://doi.org/10.1029/2021WR031721

Tian, L., Zhang, B., Chen, S., Wang, X., Ma, X., Pan, B., 2022. Large-scale afforestation enhances precipitation by intensifying the atmospheric water cycle over the Chinese Loess Plateau. Journal of Geophysical Research: Atmospheres 127, e2022JD036738. https://doi.org/10.1029/2022JD036738

Tuinenburg, O.A., Bosmans, J.H.C., Staal, A., 2022. The global potential of forest restoration for drought mitigation. Environmental Research Letters 17, 034045. https://doi.org/10.1088/1748-9326/ac55b8

van der Ent, R.J., Savenije, H.H.G., Schaefli, B., Steele-Dunne, S.C., 2010. Origin and fate of atmospheric moisture over continents. Water Resources Research 46. https://doi.org/10.1029/2010WR009127

van der Ent, R.J., Tuinenburg, O.A., Knoche, H.-R., Kunstmann, H., Savenije, H.H.G., 2013. Should we use a simple or complex model for moisture recycling and atmospheric moisture tracking? Hydrology and Earth System Sciences 17, 4869-4884. https://doi.org/10.5194/hess-17-4869-2013

van der Ent, R.J., Wang-Erlandsson, L., Keys, P.W., Savenije, H.H.G., 2014. Contrasting roles of interception and transpiration in the hydrological cycle – Part 2: Moisture recycling. Earth System Dynamics 5, 471-489. https://doi.org/10.5194/esd-5-471-2014

Wang, X., Wang, B., Xu, X., 2019. Effects of large-scale climate anomalies on trends in seasonal precipitation over the Loess Plateau of China from 1961 to 2016. Ecological Indicators 107, 105643. https://doi.org/10.1016/j.ecolind.2019.105643

Wang, X., Zhang, Z., Zhang, B., Tian, L., Tian, J., Arnault, J., Kunstmann, H., He, C., 2023. Quantifying the impact of land use and land cover change on moisture recycling with convection-permitting WRF-tagging modeling in the agro-pastoral ecotone of northern China. Journal of Geophysical Research: Atmospheres 128, e2022JD038421. https://doi.org/10.1029/2022JD038421

Wei, J., Dirmeyer, P.A., 2019. Sensitivity of land precipitation to surface evapotranspiration: a nonlocal perspective based on water vapor transport. Geophysical Research Letters 46, 12588-12597. https://doi.org/10.1029/2019GL085613

https://doi.org/10.5194/egusphere-2026-2206
Preprint. Discussion started: 4 May 2026


Woods, R., 2003. The relative roles of climate, soil, vegetation and topography in determining seasonal and long-term catchment dynamics. Advances in Water Resources 26, 295-309. https://doi.org/10.1016/S0309-1708(02)00164-1

Xie, D., Zhang, Y., Zhang, M., Tian, Y., Cao, Y., Mei, Y., Liu, S., Zhong, D., 2024. Hydrological impacts of vegetation cover change in China through terrestrial moisture recycling. Science of The Total Environment 915, 170015. https://doi.org/10.1016/j.scitotenv.2024.170015

Yan, K., Wang, J., Peng, R., Yang, K., Chen, X., Yin, G., Dong, J., Weiss, M., Pu, J., Myneni, R.B., 2024. HiQ-LAI: a high-quality reprocessed MODIS leaf area index dataset with better spatiotemporal consistency from 2000 to 2022. Earth System Science Data 16, 1601-1622. https://doi.org/10.5194/essd-16-1601-2024

Yang, D., Shao, W., Yeh, P., Yang, H., Kanae, S., Oki, T., 2009. Impact of vegetation coverage on regional water balance in the nonhumid regions of China. Water Resources Research 45. https://doi.org/10.1029/2008WR006948

Yang, Z., Dong, Q., Zhang, X., Fang, L., Zhu, X., Chen, K., Mendiondo, E.M., 2026. Interpretable Budyko-constrained machine learning framework for monthly runoff attribution in U.S. CAMELS basins. Journal of Hydrology 670, 135209. https://doi.org/10.1016/j.jhydrol.2026.135209

Yang, X., Yong, B., Ren, L., Zhang, Y., Long, D., 2017. Multi-scale validation of GLEAM evapotranspiration products over China via ChinaFLUX ET measurements. International Journal of Remote Sensing 38, 5688-5709. https://doi.org/10.1080/01431161.2017.1346400

Yang, Y., Donohue, R., McVicar, T., Roderick, M., 2015. An analytical model for relating global terrestrial carbon assimilation with climate and surface conditions using a rate-limitation framework. Geophysical Research Letters 42. https://doi.org/10.1002/2015GL066835

Yokoo, Y., Sivapalan, M., Oki, T., 2008. Investigating the roles of climate seasonality and landscape characteristics on mean annual and monthly water balances. Journal of Hydrology 357, 255-269. https://doi.org/10.1016/j.jhydrol.2008.05.010

Yosef, G., Walko, R., Avisar, R., Tatarinov, F., Rotenberg, E., Yakir, D., 2018. Large-scale semi-arid afforestation can enhance precipitation and carbon sequestration potential. Scientific Reports 8, 996. https://doi.org/10.1038/s41598-018-19265-6

Zhang, B., Tian, L., Yang, Y., He, X., 2022. Revegetation does not decrease water yield in the Loess Plateau of China. Geophysical Research Letters 49, e2022GL098025. https://doi.org/10.1029/2022GL098025

Zhang, J., Wang, S., He, Y., Ren, Y., Huang, J., 2022. Contribution of the precipitation-recycling process to the wetting trend in Xinjiang, China. Journal of Geophysical Research: Atmospheres 127, e2021JD036407. https://doi.org/10.1029/2021JD036407

Zhang, S., Yang, D., Yang, Y., Piao, S., Yang, H., Lei, H., Fu, B.-J., 2018. Excessive afforestation and soil drying on China's Loess Plateau. Journal of Geophysical Research: Biogeosciences 123. https://doi.org/10.1002/2017JG004038

Zhang, Y., Li, C., Chiew, F.H.S., Post, D.A., Zhang, X., Ma, N., Tian, J., Kong, D., Leung, L.R., Yu, Q., Shi, J., Liu, C., 2023. Southern hemisphere dominates recent decline in global water availability. Science 382, 579-584. https://doi.org/10.1126/science.adh0716

https://doi.org/10.5194/egusphere-2026-2206
Preprint. Discussion started: 4 May 2026


Zhang, Y., Zhao, X., Gong, J., Luo, F., Pan, Y., 2024. Effectiveness and driving mechanism of ecological restoration efforts
690 in China from 2009 to 2019. Science of The Total Environment 910, 168676. https://doi.org/10.1016/j.scitotenv.2023.168676